J Prosthodont Res. 2023; 67(1): 103–111

OPEN ACCESS

Journal of Prosthodontic Research

Original article

Biomechanical performance of three fiberglass post cementation techniques: Imaging, *in vitro*, and *in silico* analysis

Isis Almela Endo Hoshino [a], Paulo Henrique dos Santos [b], Andre Luiz Fraga Briso [a], Renato Herman Sundfeld [a], Satoshi Yamaguchi [c,*], Eduardo Passos Rocha [b], Rodolfo Bruniera Anchieta [a,d]

[a] Department of Preventive Dentistry and Restorative Dentistry, São Paulo State University (UNESP), School of Dentistry, Araçatuba, SP, Brazil

[b] Department of Dental Materials and Prosthodontics, São Paulo State University (UNESP), School of Dentistry, Araçatuba, SP, Brazil

[c] Department of Biomaterials Science, Osaka University Graduate School of Dentistry, Suita, Osaka, Japan

[d] Department of Prosthodontics, Centro Universitario do Norte Paulista- UNIPOS UNORP, São José do Rio Preto, SP, Brazil

Abstract

Purpose: The structural integrity of the resin cement layer, the bond strength, and the biomechanical behavior of different fiberglass post cementation techniques were evaluated.

Methods: Thirty-three bovine incisors were divided into three groups (n = 11): conventional fiberglass post (CFP), conventional fiberglass post in flared root canals (CFL), and relined fiberglass post (RFP). Six specimens from each group were submitted for high-resolution microcomputed tomography (μCT) to evaluate the integrity and presence/volume of voids at the resin cement layer. Finite element analysis (FEA) of two three-dimensional (3D) models of each group were conducted, one considered ideal (without interface defects) and another containing the conditions identified in the μCT analysis. Push-out bond strength tests were conducted for all specimens.

Results: The CFL group had the greatest mean values of void (Thirds cervical: 73.67; middle: 95.67; apical: 47.33) and gap concentration (Thirds cervical: 14.67; middle: 15.83; apical: 8.33) compared with CFP and RFP. A significant difference in bond strength was observed between the cervical (1.33 MPa) and middle thirds (1.85 MPa) compared with the apical third (4.85 MPa) of the CFL. A significant difference was observed in the bond strength in the CFL (1.33 MPa) and RFP (3.29 MPa) in the cervical third, which were statistically similar to the bond strength of the CFP. The tensile stress distributions were similar in most structures, localized in the cervical region on the lingual surface.

Conclusions: Structural defects in the interface layer might influence the bond strength and biomechanical behavior under the different fiberglass post cementations.

Keywords: Fiberglass post, Cementation, Micro CT, Porosity, Finite element analysis

Received 5 October 2021, Accepted 3 February 2022, Available online 9 March 2022

1. Introduction

The functional and aesthetic rehabilitation of teeth with endodontic involvement and significant loss of the coronary structure requires auxiliary retention and support for future restoration[1]. Fiberglass posts (FGPs) are the most commonly used intra-radicular retainers for many advantages, particular because the elastic modulus is similar to root dentin, adhesion to tooth structures and easy technique[2–4].

The main cause of failure with FGP is debonding and loosening of the post[4]. There are several factors that may increase the probability of this failure, including errors in the cementation protocol, occlusal overload, and factors related to the anatomy and characteristics of the dental remnant and post[5].

Because FGPs are prefabricated, they have an established diameter and length that vary according to their trademark, and they have limited long-term success in teeth with flared root canals and when the teeth that are repaired have extensive caries or a large anatomical variation of the canal[2,5]. The discrepancy between the diameter of the post and root canal has been reported as the main issue related to FGP loosening, a major clinical challenge in the use of these materials[6].

Under conditions in which the post is smaller than the root canal, the required cement layer may be excessively thick, which creates a weakness at the interface[3]. The large volume of cement may incorporate voids and gaps in the cement layer, creating a critical area for fault development[6]. Other factors also increase the risk of

DOI: https://doi.org/10.2186/jpr.JPR_D_21_00253

***Corresponding author:** Satoshi Yamaguchi, Department of Biomaterials Science, Osaka University Graduate School of Dentistry, 1-8 Yamadaoka, Suita, Osaka 565-0871, Japan.

E-mail address: yamaguchi.satoshi.dent@osaka-u.ac.jp

This paper is based on the master's thesis of the first author, Dr. Hoshino, published in Portuguese at the UNESP Institutional Repository on September 10, 2020.

dentin/cement/post interface failure, such as shrinkage of the resin cement while curing and a high cavity setting factor (Factor C)[7].

Various studies have evaluated aspects of FGP treatment to optimize their use, providing evaluation of uses ranging from different cementation protocols to the implementation of new techniques[1]. Among them, the technique of relining FGP with resin composite has been widely applied for its ease of use, post diameter adequacy to the root canal diameter that is related to increased frictional retention by the intimate contact of resin composite with root dentin, reduction in cement thickness, reduction in polymerization shrinkage of the cement inside the conduit, and lower incidence of voids and gaps at the interface[1,2].

Despite the promising results of this technique, the failure mechanism of relined FGP has not yet been fully elucidated, which makes it difficult to confirm its reliability in a wide root canal compared with conventional cementation[1,2].

The conventional methods used to analyze the formation of voids at the post/cement/tooth interface stand out because they are either destructive or two-dimensional tests susceptible to false positive results and without volumetric scale accuracy[8]. Three-dimensional (3D) scanning of restored specimens by microcomputed tomography (μCT) offers a non-destructive tool that is more accurate than conventional methods. The μCT provides visualization and reconstruction of the internal and external structures of the element dentistry in three dimensions, detection and measurement of the percentage of voids and gaps in the resin cement layer, and important information on the integrity of the cementation interface[2,6].

This information can be further associated with a push-out test, which increases the understanding of the bond strength between the thirds of the root canal with respect to porosity, and the different thicknesses of the cementing agent. In addition, based on the μCT data, 3D solid models could be reconstructed from which an *in silico* analysis would provide an important finding regarding the stress acting on the concentration and propagation of the failure process.

Therefore, the aim of this study was to evaluate the structural integrity of the resin cement layer, the bond strength, and the biomechanical behavior of different FGP cementation techniques in a challenging scenario with a flared root canal. The null hypotheses tested were: (1) the structural integrity of the cement/dentin interface will show no difference among the cementation techniques; (2) the bond strength will show no difference among the root thirds and the cementation techniques; and (3) the stress distribution of the cementing interface will show no difference among the three FGP cementing techniques.

2. Material and Methods

2.1. Specimen preparation

The local Ethics Committee approved this study (Protocol 00646). Thirty-three bovine incisors of similar root lengths (22 mm) and without root cracks and root curvatures were selected for the study (**Fig. 1**). Teeth were stored in distilled water at 4°C and used within three months of extraction.

To standardize the root size of the bovine incisors relative to a human incisor, the crowns at 1 mm above the cementoenamel junction (CEJ) and apical third of the roots were separated transversally to obtain a standardized root length of 16 mm. Thus, similarly sized and shaped root canals in the cervical and apical third were selected by measuring the buccolingual and mesiodistal (cervical dimensions between 3.4 and 2.0 mm; apical dimensions between 2.5 and 1.2 mm).

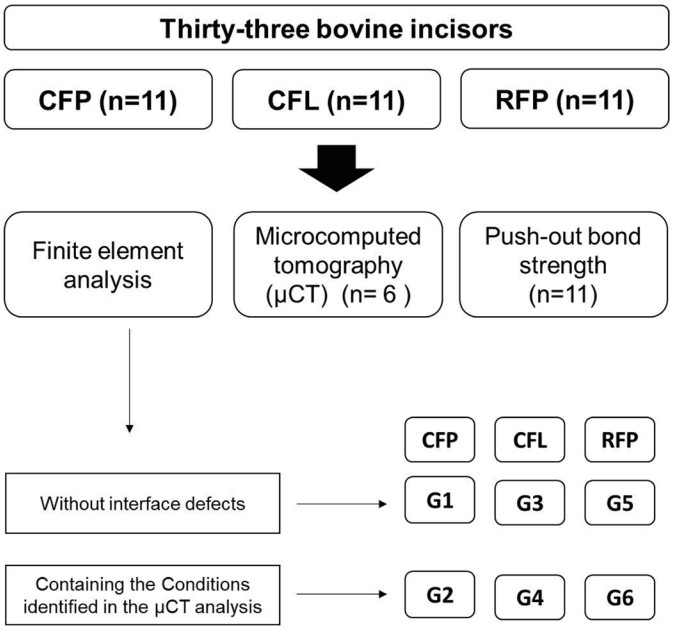

Fig. 1. Flowchart showing the distribution of groups and the analyses. The 33 teeth were divided in three groups (CFP, CFL, and RFP). Six specimens were used for μCT, and then re-used for the push-out test (n=11).

The specimens were then subjected to endodontic treatment. The Step-Back technique was used for instrumentation with a 90 to 140 K-file (Dentsply-Maillefer, Ballaigues, VD, Switzerland) at the apical foramen. Irrigation was performed with 3 mL of 2.5% sodium hypochlorite solution (NaOCl) after each file size. At the end of the preparation, a 17% EDTA solution alternating with 2.5% NaOCl was delivered into the root, followed by rinsing with distilled water. Roots were dried with absorbent paper points, filled with vertical compaction of warm gutta-percha and hydroxide-based endodontic cement (Sealer 26, Dentsply, Petrópolis, RJ, Brazil). The root access was temporarily filled with conventional glass ionomer cement (Maxxion R, FGM, Joinville, SC, Brazil) and the roots were stored under conditions of 100% relative humidity at 37°C for 72 h.

2.2. Preparation of the post space

The roots were prepared to receive fiberglass post #3 (Whitepost DC, FGM, Joinville, Brazil). The post spaces were prepared to a drilling depth of 12 mm from the sectioned surfaces, maintaining 4 mm of filling material in the apical third. The gutta-percha was removed using number 3 and 4 Gates-Glidden drill (Dentsply-Maillefer, Ballaigues, VD, Switzerland). The corresponding drill of post #3, corresponding to the diameter of the post, was used to ensure a perfect fit in the post space.

Twenty-two specimens were flared between the middle and cervical thirds of the root with a #730 conical diamond bur (KG So-

rensen, Cotia, SP, Brazil) with 5.5 mm crown diameter adapted in a low-speed handpiece. The diamond bur was introduced parallel and centered in the root canal, with a working length of up to 8 mm, taking the most coronary tooth surface as a reference.

After the preparations, the root canals were irrigated with 2.5% NaOCl and 17% EDTA solutions to remove the smear layer. The root canals were then cleaned with distilled water and dried with absorbent paper points.

2.3. Post cementation

The specimens were divided into three experimental groups (n = 11) as follows.

2.3.1. CFP: Conventional fiberglass post (Positive control group)

This group simulated an ideal adaptation of the post. The fiberglass posts #3 with a diameter compatible with the root canal were cemented into the roots. Before cementation, the posts were placed into the root canal to confirm the position and adaptation through digital radiographs. Then, the posts surface was cleaned with 70% ethanol and conditioned using 35% phosphoric acid for 20 s, then silanized (Prosil, FGM, Joinville, SC, Brazil) for 1 min. Self-adhesive cement (RelyX U200, 3M ESPE, St Paul, MN, United States) coupled to a mixing root canal tip was prepared. The tip was introduced into the root canal and the cement was injected so that the post space was filled. The post was introduced into the post space and excess material was removed. Finally, the cement was cured with a LED curing light with a radiant emittance of 1000 mW/cm^2. (VALO® Cordless, Ultradent, South Jordan, UT, United States) directed at the occlusal surface for 40 s.

2.3.2. CFL: Conventional fiberglass post in flared root canals

The same procedures used for the CFP group were performed; however, an inadequate adaptation of the post using teeth with flared root canals was used.

2.3.3. RFP: Relined fiberglass post

In this group, FGP relined with resin composite in flared root canals was used[1]. The post surface was prepared as described in the CFP group and it was then relined with resin composite (Z350 XT, 3M ESPE, St Paul, MN, USA), and the post space was lubricated using a water-based gel (KY, Johnson & Johnson, Sao Jose dos Campos, SP, Brazil). The relined FGP was inserted into the post space, and the coronary part of the post was polymerized for 20 s. The post was then removed from the post space and polymerized for another 40 s, with the light-curing device positioned over the resin composite and light curing throughout its extension. Before the cementation, the relined post surface was cleaned using 35% phosphoric acid for 20 s and the root canal was washed with water and dried with paper cones. Using an intracanal mixing tip, the self-adhesive cement (RelyX U200) was injected into the post space and the relined FGP was inserted and polymerized for 40 s through the occlusal face.

2.4. Structural analysis by microcomputed tomography (μCT)

For evaluation of the structural integrity, volume, and the presence of voids at the resin cement layer, six specimens from each group were analyzed using high-resolution microcomputed tomography (μCT) (SkyScan 1272, Kontich, Belgium)[2].

Specimens were scanned immediately after the restorative procedures were concluded. The resolution was 13 μm with an exposure time of 3 s. The scanning was performed by 180° rotation around the vertical axis with a rotation step of 0.4 with a 1 mm Al filter. The resulting images were reconstructed using NRecon software (SkyScan) that produced 2-dimensional (2D) slices of the inner structure of the filled roots. CTAn and CTVol software (DataViewer, SkyScan) were used for volumetric analysis and to render 3D models of the roots. The total volume of the root canal, the volume of the voids/gaps within the root canal, and the percentage volume of voids was measured in each sample[2].

2.5. Push-out bond strength test

The remaining teeth were stored for 7 months in distilled water, and the solution was changed every 7 days. After this time, the specimens were sectioned perpendicular to the long axis. For each specimen, a slice of 1 mm was obtained from each third to be analyzed (i.e., cervical, middle, and apical).

A push-out test was conducted using an universal loading device (DL3000, Emic, Sao Jose Dos Pinhais, PR, Brazil) with a 1 kN load cell at a crosshead speed of 0.5 mm/min. The load was applied in the apical coronal direction until the post was dislodged or the specimen fractured[9].

The bond strength values for the push-out test were calculated as follows[10]:

$$Ru = F / A,$$

where *Ru* (bond strength) is the division of the maximum force (*F*) by the interface area (*A*). To determine the area of the union interface, the following formula was applied:

$$A = \pi(r1+r2)\sqrt{(r1-r2)^2 + h^2},$$

where (*h*) is the height of the post, π is 3.14, (*r1*) is the largest radius, and (*r2*) is the smallest radius. The values of *r1* and *r2* correspond to the radius of the inner diameter of the root canal walls obtained by measuring the internal diameter of the major and minor base.

Qualitative fractographic analysis was also performed on all specimens, primarily using stereo polarized light microscopy and bilateral (DISCOVERY V20, Carl Zeiss, Oberkochen, Germany) 40× magnification with illumination to determine the type of fracture[11]. Fractures were classified as: **A.** Cohesive fracture in the dental substrate, **B.** Cohesive fracture in cement, **C.** Adhesive fracture, and **D.** Mixed fracture (i.e., adhesive interface fracture with cohesive dentin and/or resin cement involvement).

Representative specimens from each group were coated with gold (Emitech K650, Emitech Products Inc., Houston, TX, USA) for scanning electron microscopy (SEM, EVO LS-15, Carl Zeiss) to characterize different failure patterns after the bonding test.

Table 1. Mechanical properties of isotropic materials and resin cement in finite element models with structural defects for each group. Elastic modulus (E) and Poisson's ratio (γ).

Materials	E (GPa)	Ref.	γ	Ref.
Enamel	35.2	Bechtle *et al*. 2010	0.33	Li *et al*. 2009
Dentin	14.56	Bechtle *et al*. 2010	0.32	Li *et al*. 2009
Periodontal ligament	6.89×10^{-5}	Yettram *et al*. 1977	0.45	Okamoto *et al*. 2008
Gutta-percha	1.4×10^{-1}	Friedman *et al*. 1975	0.45	Friedman *et al*. 1975
Resin Cement	8.3	Okamoto *et al*. 2008	0.30	Okamoto *et al*. 2008
Composite Resin	16.6	Okamoto *et al*. 2008	0.24	Okamoto *et al*. 2008
Lithium Disilicate	65	Li *et al*. 2009	0.24	Li *et al*. 2009
Resin cement with voids and gaps of G2	8.1747	Calculated with μCT data and homogenization analysis	0.299	Calculated with μCT data and homogenization analysis
Resin cement with voids and gaps of G4	8.2999	Calculated with μCT data and homogenization analysis	0.3	Calculated with μCT data and homogenization analysis
Resin cement with voids and gaps of G6	8.2859	Calculated with μCT data and homogenization analysis	0.299	Calculated with μCT data and homogenization analysis

2.6. *In silico finite element analysis*

Based on the μCT analysis and optical microscopy images (DISCOVERY V20, Carl Zeiss), a representative specimen from each experimental group (CFP, CFL, and RFP) was used to elaborate the 3D models. Photomicrographs of one sectioned specimen from each group were produced to obtain more reliable 3D models of the central incisor anatomy. Optical microscopy images was obtained from three specimen (CFP, CFL, and RFP), in order to help the 3D model built. The average thickness of the resin cement layer in the cervical, middle, and apical thirds of the CFL was 1.56 nm, 0.41 nm, and 0.32 mm, respectively. The thickness of the CFL was relatively larger than CFP and RFP, which had an average thickness (cervical, middle, and apical thirds) of 0.32 mm, 0.27 mm, and 0.25 mm, and 0.22 mm, 0.13 mm, and 0.17 mm, respectively.

The voids and gaps data from the μCT analysis were obtained by processing the image slices of each specimen (incisal to apical direction) and calculating the overall mean for each specimen group. The integrity of the resin cement layer, the locations of the voids, and the thickness of the cement layer were also considered in the confection of the 3D models.

Two models were designed for each group: an ideal model (without interface defect), and a model containing the conditions identified during the μCT analysis. The data obtained were converted to Digital Imaging and Communications in Medicine (DICOM) files and exported to SolidWorks 2011 software (SolidWorks Corp., MA, United States) for model reconstruction. All of the structures (enamel, dentin, periodontal ligament, gutta-percha, fiber post, resin composite, and cement) were recognized and included in the solid models. A ceramic crown was separately modeled and included in the base 3D model of each group.

The mechanical properties (elastic modulus [E] and Poisson's ratio [γ]) of all model structures were obtained from specific literature (**Table 1**)[12–16]. The FGP was considered orthotropic, homogeneous, and linearly elastic (**Table 2**)[17].

Multi-scale analysis was conducted to improve the stress analysis at the post/cement/dentin interface using voxelization of the models[18,19]. The resulting models were homogenized, and mechanical properties at macro-scale were obtained based on the level of defects of each interface tested.

Table 2. Orthotropic Properties of fiberglass post (Lanza et al. 2005)

Elastic modulus (GPa)	Poisson's ratio	Shear Module (G)
X=37	Xy=0.27	Gxy=3.1
Y=9.5	Xz=0.34	Gxz=3.5
Z=9.5	Yz=0.27	Gyz=3.1

Therefore, based on the information discovered from quantification of the structural defects, a micro-scale model of a 1×1×1 mm^2 resin cement block was made containing the volume and mean diameter of the voids identified using μCT (i.e., G2 = Φ0.245 mm, G4 = Φ0.017 mm, and G6 = Φ0.117 mm) (**Fig. 2**).

This micro-scale model was exported to VOXELCON2015 software (Quint Corporation., Fuchu, Tokyo, Japan) for FEA and enhancement in this region (**Fig. 2**). The voxel size varied in relation to the void diameter. After refinement, the micro-scale models were homogenized and the elastic modulus and Poisson's ratio at macro-scale were acquired through mathematical calculations considering the level of interface defects (**Table 1**).

These characteristics were then reflected to the macro-scale models, and a distributed load of 180 N was applied to the lingual surface, in the incisal third, 45° to the long axis of the tooth for all models[20]. The external surface of the periodontal ligament was fixed on the X, Y, and Z axes for all models. FEA was conducted using SolidWorks 2011 software to obtain the maximum principal stresses.

2.7. *Statistical analysis*

The mean values of the amount and volume of the voids and gaps in the cement layer, as well as the push-out result for each group, were calculated and were submitted to the normality curve adherence (Shapiro–Wilk) test. The voids/gaps formation and bond strength variable presented a normal distribution. Two-way analysis of variance (ANOVA) and Tukey's post-hoc test (α = 0.05) were performed.

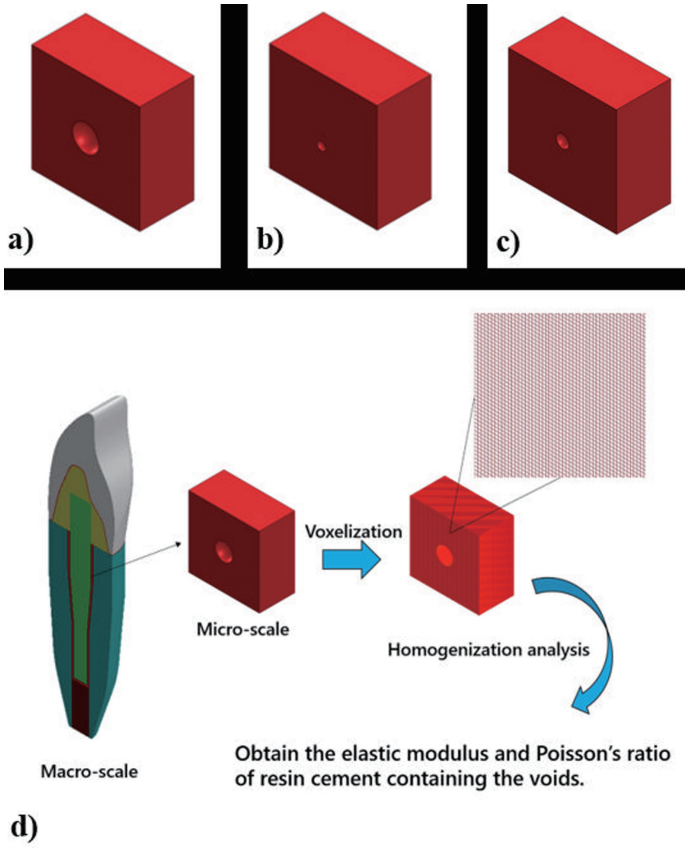

Fig. 2. Illustration of the microscale voids used in finite element models with structural defects. The volume and mean diameter of the voids identified in microtomography for each group were used for the voxelization process: a. G2 = Φ0.245 mm; b. G4 = Φ0.017 mm; c. G6 = Φ0.117 mm. d. Voxelization process and improvement of the finite element mesh in the structural defect model (G2). The elastic modulus and Poisson's ratio of the resin cement layer was obtained for each group using homogenization analysis.

3. Results

3.1. μCT analysis

Regarding the concentration of voids in the cement layer (**Table 3**), there were only statistical differences between the middle and apical root thirds in CFL ($p < 0.05$). The void concentration was significantly greater in CFL, with statistical differences with CFP and RFP among all the root thirds ($p < 0.05$).

The volume of the voids is shown in **Table 3**. CFL and RFP showed a statistical difference between the cervical third and middle and apical thirds, within groups ($p < 0.05$). This difference was not observed among the root thirds of the CFP. Comparing the groups, the only statistically significant difference was between the middle and apical thirds of the CFP and those of CFL and RFP, and the voids were significantly larger in CFP ($p < 0.05$). The voids occurred predominantly on the buccal surface in all groups (**Fig. 3**). In CFL, the voids were closer to the interface than with CFP and RFP.

The results of the gap quantification (**Table 4**) showed statistically significant differences between the middle third and apical third of the CFL and between the cervical and middle third with the apical third of the RFP ($p < 0.05$). In the comparison of groups, the gap concentration was significantly greater for CFL, with statistical differences with CFP and RFP, among all root thirds ($p < 0.05$).

The results of the gap volume in **Table 4** indicate that there was no difference among the analyzed groups or thirds.

Gaps were observed predominantly on the lingual surface between the post and cement layer for CFP and RFP groups. For CFL, the gaps occurred more on the buccal surface between the cement layer and the intra-radicular dentin.

3.2. Push-out analysis

Table 5 shows the statistical difference between the cervical and middle thirds, and the apical third in CFL ($p < 0.05$). In the comparison of the groups, there was a statistical difference in the cervical thirds of CFL and RFP ($p < 0.05$), both statistically similar to CFP.

In the fractography analysis (**Fig. 4**), the fracture pattern observed in the groups was mostly adhesive (CFP 56.66%; CFL 46.66%), except for RFP in which the adhesive fracture and cohesive fracture in the substrate were similar (40%) (**Table 5**).

3.3. Finite element analysis

When comparing cementation techniques (**Table 6**), the maximum values of maximum principal stress (tensile stress) were observed in the cervical region on the palatal face for all groups (**Fig. 5**) in all simulated models. In the 3D analysis in the macro-scale models, the maximum principal stress levels of the G1 and G5 cement layer specimens were 275.6 and 271.1 MPa, respectively, greater than G2 and G6 (268.4 and 270.9 MPa, respectively). The stress levels in G3 and G4 were similar in the cement layer.

4. Discussion

Failures in the integrity of the resin cement layer were observed in all groups and differences in bond strength at all root canal levels. In particular, CFL showed excessive formation of voids and gaps in the cement layer and the lowest bond strength. Based on these re-

Table 3. Mean and standard deviation of quantification and volume of voids in the cement layer (mm^3)

	Quantification of voids			Volume of voids		
	CFP	CFL	RFP	CFP	CFL	RFP
Cervical	10.00 ± 4.98 A b	73.67 ± 25.41 AB a	10.83 ± 36.6 A b	3.73 ± 3.13 A a	3.19 ± 0.61 A a	3.83 ± 0.70 A a
Middle	10.67 ± 4.46 A b	95.67 ± 29.55 A a	13.33 ± 7.94 A b	5.37 ± 3.44 A a	1.70 ± 0.35 B b	2.27 ± 1.08 B ab
Apical	6.67 ± 4.46 A b	47.33 ± 14.22 B a	5.67 ± 2.50 A b	4.84 ± 3.12 A a	2.73 ± 3.42 B b	1.19 ± 0.26 B b

Different letters indicate statistically significant difference (p<0.05). Uppercase letters (vertical) compare root thirds in the same group and lowercase letters (horizontal) compare FGP cementation techniques on the same root third.

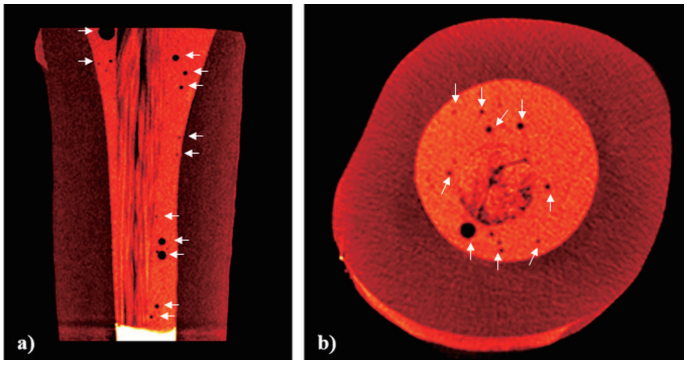

Fig. 3. Microcomputed tomographic image of the structural defects in the cement layer. **a.** 3D model of the CFL group with longitudinal section showing the voids and gaps in the cement layer. **b.** Image of the cervical region of the CFL group showing the distribution of the voids in the cement layer. Arrows represent the voids inside the resin cement layer.

sults, the first and second null hypotheses were rejected.

In addition to the thicker cement layer in the CFL, which makes it more prone to void formation because of the large amount of resinous material[21,22], there is more polymerization shrinkage. This is especially true in the cervical and middle thirds, which may explain the greater gap formation in the cementation line and consequent reduction in the contact area between the resin cement and root dentin[23,24].

Thus, although some studies suggest that increasing the thickness of the resin cement around FGP is not detrimental to post installation performance and bond strength[25], the opposite was observed in the present study. The geometric configuration of the root canal combined with the high volume of resin cement increased the occurrence of failure in the cement layer increased and negatively affected the bond strength[26],[7]. Additionally, the bond strength can also be influenced by the location of these structural defects because the distribution of voids and gaps is not uniform across the cementing layer, regardless of the group[27]. Similarly, the higher incidence of these defects in the cement layer increased the dissolution and degradation levels of the material, resulting in decreased post installation retention[10], making it possible to assume a predisposition to adhesive fracture in the mechanical test, as observed in the analyses.

Another aspect that should be considered in this study is the interaction of the resin cement functional monomers (4-methacryloxyethyl trimellitic acid monomers and phosphoric acid esters) with the external surface of the post[28,29], which can interfere with the bond strength and contribute to more structural defects between the post and cement, as observed in CFP. To ensure this interaction and increase the adhesion of silica-based materials, different surface treatment protocols have been proposed[28,30,31], with the application of silane bonding agents most common[28,32,33].

Silane has a bifunctional organic structure with two reactive ends, which, after hydrolyzation of its components at low pH[32], promote the formation of chemical tips between the glass phase of the post and the resin matrix of the cement[34]. Although some results show that silane effectively promotes the adhesion of silica-based materials, such as FGP[34,35], the use of pre-hydrolyzed single-vial silane solutions (such as used in this study) may be less effective than other materials used in the form of unhydrolyzed solutions in double vials because of instability of the final solution[34].

Corroborating the findings of other studies[10,36], RFP allowed the formation of a more homogeneous and relatively thin cementation line, making the observation of structural defects at the interface difficult[2,22]. The intimate contact of the post/resin composite/cement with the root canal walls is believed to promote micromechanical adhesion and greater frictional retention[3,37], which explains the excellent performance in the bond strength analysis of this group.

Table 4. Mean and standard deviation of quantification of gaps at the cement/dentin and cement/post interface and their volume (mm^3)

	Quantification of gaps			Volume of gaps		
	CFP	CFL	RFP	CFP	CFL	RFP
Cervical	2.83 ± 1.17 A b	14.67 ± 5.35 AB a	4.00 ± 1.67 A b	3.55 ± 1.29 A a	2.91 ± 3.47 A a	4.00 ± 1.14 A a
Middle	2.33 ± 1.03 A b	15.83 ± 5.12 A a	3.33 ± 1.35 A b	5.26 ± 2.29 A a	3.52 ± 2.94 A a	3.09 ± 1.33 A a
Apical	1.83 ± 0.41 A b	8.33± 3.01 B a	1.33 ± 0.52 B b	2.28 ± 2.24 A a	2.39 ± 1.88 A a	3.68 ± 2.89 A a

Different letters indicate statistically significant difference ($p<0.05$). Uppercase letters (vertical) compare root thirds in the same group and lowercase letters (horizontal) compare FGP cementation techniques on the same root third.

Table 5. Mean and standard deviation of push-out bond strength (MPa) and the percentage of each type of fracture found in the fractographic analysis

	CFP	CFL	RFP
Cervical	2.27±1.04 A ab	1.33±1.19 B b	3.29±2.38 A a
Middle	4.73±4.63 A a	1.85±1.59 B a	4.51±2.37 A a
Apical	4.65±2.30 A a	4.85±2.38 A a	4.84±2.37 A a
Cohesive fracture in the dental substrate	16.66%	26.66%	40%
Cohesive fracture in cement	6.67%	6.67%	3.33%
Adhesive fracture	56.67%	46.67%	40%
Mixed fracture	20%	20%	16.67%

Distinct uppercase letters (vertical) compare root thirds in the same group, and lowercase letters (horizontal) compare fiberglass post cementation techniques in the same root third, with statistically significant differences ($p<0.05$).

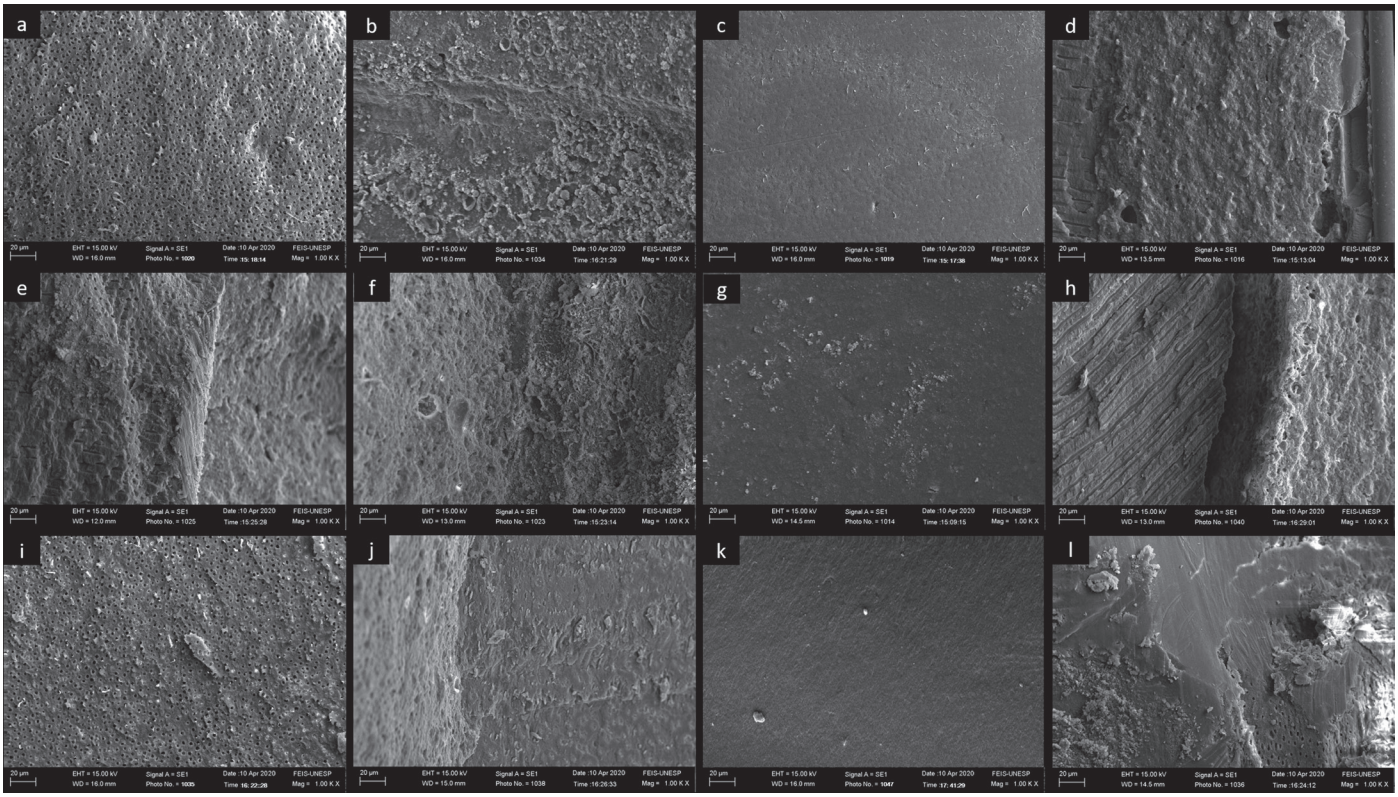

Fig. 4. Scanning electron microscopy images of fractured specimens for each group: **a.** Cohesive fracture in the dental substrate in the CFP group; **b.** Cohesive fracture in cement in the CFP group; **c.** Adhesive fracture in the CFP group; **d.** Mixed fracture in the CFP group; **e.** Cohesive fracture in the dental substrate in the CFL group; **f.** Cohesive fracture in cement in the CFL group; **g.** Adhesive fracture in the CFL group; **h.** Mixed fracture in the CFL group; **i.** Cohesive fracture in the dental substrate in the RFP group; **j.** Cohesive fracture in cement in the RFP group; **k.** Adhesive fracture in the RFP group; **l.** Mixed fracture in the RFP group. WD 13-16mm, Mag =1000×; 15Kv.

Table 6. Distribution maximum stress levels (MPa)

	D	F	CL	T	CI	C
G1	198.5	8.0	5.5	22.0	275.6	237.7
G2	194.5	3.7	3.5	22.0	268.4	230.8
G3	189.9	5.5	14.8	22.9	273.3	236.0
G4	189.9	5.5	14.8	22.9	273.3	236.0
G5	196.1	5.8	14.0	22.3	271.1	232.9
G6	195.9	5.8	14.0	22.3	270.9	232.8

D-Dentin; CL- Post cement layer; F- Fiberglass post; T- Composite resin trunnion; CI- Crown cementing interface; C- Crown.

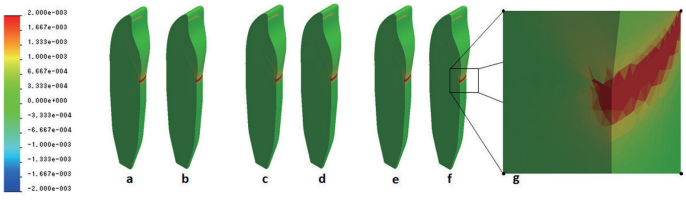

Fig. 5. Maximum principal stress maps of each group. The peak of stress occurred at the enamel–dentin junction on the palatine face for all groups. The stress distribution behavior was similar in all groups: model with **a**. ideal interface in G1 (CFP), **b.** structural defects in G1 (CFP), **c.** ideal interface in G3 (CFL), **d.** structural defects in G4 (CFL), **e.** ideal interface in G5 (RFP), and **f.** structural defects in G6 (RFP); **g.** represents the magnification of the peak stress level.

Some studies identified that the apical region is pre-disposed to more cement/dentin interface failures and a lower bond strength because of difficult access and cleaning, and reduced light diffusion capacity in this region. These conditions result in inhomogeneous distribution of the apical region material and lower conversion of the resin cement monomers[5]. In contrast, there are also studies describing that limited light access in this region did not result in incomplete polymerization and may be considered an advantage when using double-cured resin cement. It is possible to assume that the shrinkage stresses of resin cement in this root third are minimal[22]. In addition, the apical third of a root canal has the smallest diameter when compared with the cervical and middle thirds, which provides a tighter post even on teeth with a flared root canal. Thus, as observed in this study, the formation of a thin layer of cement and lower incidence of voids and gaps contributed to the good performance in this root third[22].

The FEA simulations of the mechanical behavior demonstrated different patterns in the stress levels at the cement/post interface with the conventional technique and in the post relined using the resin composite technique. Thus, the third null hypothesis that there would be no difference in the stress distribution of the cementation interface among the three FGP cementation techniques was rejected. Despite the results of this study, the difference in stress in the resin cement layer between the models does not necessarily indicate

that a defective resin cement layer is less susceptible to failure than a defect-free layer[14,20].

In the G1 model with the resin cement layer of ideal characteristics, the lower deformation of the cement layer, associated with the friction between resin cement and dentin, generated higher stress concentrations in the cement layer[1] compared with G2. These stresses were exacerbated along the post and within the root canal because the canal walls could not compensate for stresses by deformation or elastic compliance[7]. In contrast, in G2, the cement layer underwent the greatest deformation under the same load. This deformation occurred because of voids, which are hollow structural defects, and because of the low elastic modulus and Poisson's ratio in the cement layer of this model[1]. Therefore, despite the lower stress levels in G2, compared with G1, G2 is more susceptible to structural failure because the defective cement layer reaches the breaking point under low stress.

Despite a thicker layer and higher void concentration, CFL group models indicated the smallest volume of voids, thus represented in the finite element models with the lowest percentage of cement layer voids per square millimeter. This did not considerably change the elastic modulus of the cement layer from G3 to G4.

As a non-destructive tool, μCT provides important data about the integrity of the resin cement layer. High-precision 3D analysis allowed complementary tests[2,6,38], such as the bond strength and finite element analysis, to be better elucidated.

The results obtained in this study clarified the mechanism of failure of joining teeth restored with FGP in the challenging setting of a wide root canal. Moreover, the results indicate that the FGP relining technique is an excellent clinical alternative. However, some limitations of the study need to be considered. The incidence of unidirectional and static loading, represented by the extrusion micro shear test and FEA, do not represent the multiaxial and repetitive conditions to which a tooth is exposed during masticatory function[39]. Performing the step-stress accelerate life test progressive accelerated fatigue test (SSALT), combined with computational imaging and multi-scale simulation techniques, might show the damaging cumulative effect of fatigue on interface defects, extending the potential for extrapolating these results to clinical practice[40–43].

5. Conclusions

Structural defects at the interface reduce the bond strength; however, homogenization analysis of these defects clarified that they are also stress escape regions of the biomechanical behavior under different FGP cementation techniques. For teeth with flared root canals, FGP relined with a resin composite technique provided a relatively thin, homogeneous cementation line with fewer structural defects that resulted in good stress distribution and a greater bond strength than conventional techniques.

Acknowledgments

The authors thank FOA-UNESP's Multiuser Laboratory (São Paulo State University -UNESP, School of Dentistry, Brazil) for technical support in performing the computed microtomography analysis (SkyScan 1272). The authors also thank the São Paulo Research Foundation - FAPESP (2018/17980-1) for funding this analysis. The authors thank Ana Teresa Maluly-Proni for her collaboration in execution the analysis push out. This research was supported by a Grant-in-Aid for Scientific Research (No. JP19K10244) from the Japan Society for the Promotion of Science (JSPS). We thank Ashleigh Cooper, PhD, from Edanz Group (https://en-author-services.edanz.com/ac) for editing a draft of this manuscript.

Conflicts of interest

The authors have declared that no conflict of interest exists.

References

[1] Faria-e-Silva AL, Pedrosa-Filho Cde F, Menezes Mde S, Silveira DM, Martins LR. Effect of relining on fiber post retention to root canal. J Appl Oral Sci. 2009;17:600-4.

[2] Caceres EA, Sampaio CS, Atria PJ, Moura H, Giannini M, Coelho PG, *et al.* Void and gap evaluation using microcomputed tomography of different fiber post cementation techniques. J Prosthet Dent. 2018;119:103–7. https://doi.org/10.1016/j.prosdent.2017.01.015, PMID:28461048

[3] Lazari PC, Oliveira RC, Anchieta RB, Almeida EO, Freitas Junior AC, Kina S, *et al.* Stress distribution on dentin-cement-post interface varying root canal and glass fiber post diameters. A three-dimensional finite element analysis based on micro-CT data. J Appl Oral Sci. 2013;21:511-7.

[4] Frydman G, Levatovsky S, Pilo R. [Fiber reinforced composite posts: literature review]. Refu'at ha-peh veha-shinayim (1993) 2013;30:6-14, 60.

[5] Daleprane B, Pereira CNB, Bueno AC, Ferreira RC, Moreira AN, Magalhães CS. Bond strength of fiber posts to the root canal: effects of anatomic root levels and resin cements. J Prosthet Dent. 2016;116:416–24. https://doi.org/10.1016/j.prosdent.2016.01.030, PMID:27086107

[6] Uzun İH, Malkoç MA, Keleş A, Öğreten AT. 3D micro-CT analysis of void formations and push-out bonding strength of resin cements used for fiber post cementation. J Adv Prosthodont. 2016;8:101–9. https://doi.org/10.4047/jap.2016.8.2.101, PMID:27141253

[7] Tay F, Loushine R, Lambrechts P, Weller R, Pashley D. Geometric factors affecting dentin bonding in root canals: a theoretical modeling approach. J Endod. 2005;31:584–9. https://doi.org/10.1097/01.don.0000168891.23486.de, PMID:16044041

[8] Nazari A, Sadr A, Shimada Y, Tagami J, Sumi Y. 3D assessment of void and gap formation in flowable resin composites using optical coherence tomography. J Adhes Dent. 2013;15:237–43. PMID:23534012

[9] Bakaus TE, Gruber YL, Reis A, Gomes OMM, Gomes GM. Bond strength values of fiberglass post to flared root canals reinforced with different materials. Braz Oral Res. 2018;32:e13. https://doi.org/10.1590/1807-3107bor-2018.vol32.0013, PMID:29513887

[10] Farid F, Rostami K, Habibzadeh S, Kharazifard M. Effect of cement type and thickness on push-out bond strength of fiber posts. J Dent Res Dent Clin Dent Prospect. 2018;12:277–82. https://doi.org/10.15171/joddd.2018.043, PMID:30774794

[11] Le Bell AM, Tanner J, Lassila LV, Kangasniemi I, Vallittu P. Bonding of composite resin luting cement to fiber-reinforced composite root canal posts. J Adhes Dent. 2004;6:319–25. PMID:15779318

[12] Bechtle S, Fett T, Rizzi G, Habelitz S, Klocke A, Schneider GA. Crack arrest within teeth at the dentinoenamel junction caused by elastic modulus mismatch. Biomaterials. 2010;31:4238–47. https://doi.org/10.1016/j.biomaterials.2010.01.127, PMID:20167362

[13] Friedman CM, Sandrik JL, Heuer MA, Rapp GW. Composition and mechanical properties of gutta-percha endodontic points. J Dent Res. 1975;54:921–5. https://doi.org/10.1177/00220345750540052901, PMID:1058875

[14] Liu HL, Lin CL, Sun MT, Chang YH. Numerical investigation of macro- and micro-mechanics of a ceramic veneer bonded with various cement thicknesses using the typical and submodeling finite element approaches. J Dent. 2009;37:141–8. https://doi.org/10.1016/j.jdent.2008.10.009, PMID:19084316

[15] Okamoto K, Ino T, Iwase N, Shimizu E, Suzuki M, Satoh G, *et al.* Three-dimensional finite element analysis of stress distribution in composite resin cores with fiber posts of varying diameters. Dent Mater J. 2008;27:49–55. https://doi.org/10.4012/dmj.27.49, PMID:18309611

[16] Yettram AL, Wright KWJ, Houston WJB. Centre of rotation of a maxillary central incisor under orthodontic loading. Br J Orthod. 1977;4:23–7. https://doi.org/10.1179/bjo.4.1.23, PMID:273433

[17] Lanza A, Aversa R, Rengo S, Apicella D, Apicella A. 3D FEA of cemented steel, glass and carbon posts in a maxillary incisor. Dental materials. 2005;21:709-15.

[18] Lee C, Yamaguchi S, Ohta K, Imazato S. Mechanical properties of computer-aided design/computer-aided manufacturing resin composites assuming perfect silane coupling using in silico homogenization of cryo-electron microscopy images. J Prosthodont Res. 2019;63:90–4. https://doi.org/10.1016/j.jpor.2018.09.001, PMID:30529229

[19] Yamaguchi S, Inoue S, Sakai T, Abe T, Kitagawa H, Imazato S. Multi-scale analysis of the effect of nano-filler particle diameter on the physical properties of CAD/CAM composite resin blocks. Comput Methods Biomech Biomed Engin. 2017;20:714–9. https://doi.org/10.1080/10255842.2017.1293664, PMID:28387166

[20] Anchieta RB, Rocha EP, Almeida EO, Freitas Junior AC, Martin Junior M, Martini AP, *et al.* Influence of customized composite resin fibreglass posts on the mechanics of restored treated teeth. Int Endod J. 2012;45:146–55. https://doi.org/10.1111/j.1365-2591.2011.01955.x, PMID:22070803

[21] Chang YH, Wang HW, Lin PH, Lin CL. Evaluation of early resin luting cement damage induced by voids around a circular fiber post in a root canal treated premolar by integrating micro-CT, finite element analysis and fatigue testing. Dental materials. 2018;34:1082-8.

[22] D'Arcangelo C, Cinelli M, De Angelis F, D'Amario M. The effect of resin cement film thickness on the pullout strength of a fiber-reinforced post system. J Prosthet Dent. 2007;98:193–8. https://doi.org/10.1016/S0022-3913(07)60055-9, PMID:17854620

[23] Anchieta RB, Machado LS, Hirata R, Coelho PG, Bonfante EA. Survival and failure modes: platform-switching for internal and external hexagon cemented fixed dental prostheses. Eur J Oral Sci. 2016;124:490–7. https://doi.org/10.1111/eos.12298, PMID:27680671

[24] Silva NR, Aguiar GCR, Rodrigues MP, Bicalho AA, Soares PBF, Veríssimo C, *et al.* Effect of Resin Cement Porosity on Retention of Glass-Fiber Posts to Root Dentin: An Experimental and Finite Element Analysis. Braz Dent J. 2015;26:630–6. https://doi.org/10.1590/0103-6440201300589, PMID:26963208

[25] Perez BE, Barbosa SH, Melo RM, Zamboni SC, Ozcan M, Valandro LF, *et al.* Does the thickness of the resin cement affect the bond strength of a fiber post to the root dentin? Int J Prosthodont. 2006;19:606–9. PMID:17165301

[26] Versluis A, Tantbirojn D, Pintado MR, DeLong R, Douglas WH. Residual shrinkage stress distributions in molars after composite restoration. Dental materials. 2004;20:554-64.

[27] Yikilgan I, Uzun O, Gurel M, Bala O, Omurlu H, Kayaoglu G. Volumetric Evaluation of Void/Gap Formation and Microleakage Cementing Fiber Posts on Extracted Teeth with Three Different Cements. J Prosthodont. 2019;28:e222-e8.

[28] Prado M, Marques JN, Pereira GD, da Silva EM, Simão RA. Evaluation of different surface treatments on fiber post cemented with a self-adhesive system. Mater Sci Eng C. 2017;77:257–62. https://doi.org/10.1016/j.msec.2017.03.141, PMID:28532027

[29] Simões TC, Luque-Martinez ÍV, Moraes RR, Sá ATG, Loguercio AD, Moura SK. Longevity of Bonding of Self-adhesive Resin Cement to Dentin. Oper Dent. 2016;41:E64–72. https://doi.org/10.2341/14-266-LR, PMID:26918926

[30] Chen Q, Wang XZ. [Evaluation of modified micro-push-out bond strength of glass fiber posts with chemically treated resin cements]. Beijing da xue xue bao Yi xue ban. 2019;51:968-72.

[31] Shafiei F, Saadat M, Jowkar Z. Effect of laser heat treatment on Pull-out bond strength of fiber posts treated with different silanes. J Clin Exp Dent. 2018;10:e413–8. PMID:29849963

[32] Perdigao J, Gomes G, Lee IK. The effect of silane on the bond strengths of fiber posts. Dental materials. 2006;22:752-8.

[33] Rathke A, Haj-Omer D, Muche R, Haller B. Effectiveness of bonding fiber posts to root canals and composite core build-ups. Eur J Oral Sci. 2009;117:604–10. https://doi.org/10.1111/j.1600-0722.2009.00668.x, PMID:19758259

[34] Lung CY, Matinlinna JP. Aspects of silane coupling agents and surface conditioning in dentistry: an overview. Dental materials. 2012;28:467-77.

[35] Matinlinna JP, Lung CYK, Tsoi JKH. Silane adhesion mechanism in dental applications and surface treatments: A review. Dental materials. 2018;34:13-28.

[36] Farina AP, Chiela H, Carlini-Junior B, Mesquita MF, Miyagaki DC, Randi Ferraz CC, *et al.* Influence of Cement Type and Relining Procedure on Push-Out Bond Strength of Fiber Posts after Cyclic Loading. J Prosthodont. 2016;25:54-60.

[37] Goracci C, Fabianelli A, Sadek F, Papacchini F, Tay F, Ferrari M. The contribution of friction to the dislocation resistance of bonded fiber posts. J Endod. 2005;31:608–12. https://doi.org/10.1097/01.don.0000153841.23594.91, PMID:16044046

[38] Lorenzoni FC, Bonfante EA, Bonfante G, Martins LM, Witek L, Silva NR. MicroCT analysis of a retrieved root restored with a bonded fiber-reinforced composite dowel: a pilot study. J Prosthodont. 2013;22:478-83.

[39] Braga RR, Ballester RY, Ferracane JL. Factors involved in the development of polymerization shrinkage stress in resin-composites: a systematic review. Dental materials. 2005;21(10):962-70.

[40] Bonfante EA, Coelho PG, Guess PC, Thompson VP, Silva NRFA. Fatigue and damage accumulation of veneer porcelain pressed on Y-TZP. J Dent. 2010;38:318–24. https://doi.org/10.1016/j.jdent.2009.12.004, PMID:20026232

[41] Coelho PG, Bonfante EA, Silva NRF, Rekow ED, Thompson VP. Laboratory simulation of Y-TZP all-ceramic crown clinical failures. J Dent Res. 2009;88:382–6. https://doi.org/10.1177/0022034509333968, PMID:19407162

[42] Coelho PG, Silva NR, Bonfante EA, Guess PC, Rekow ED, Thompson VP. Fatigue testing of two porcelain-zirconia all-ceramic crown systems. Dental materials. 2009;25:1122-7.

[43] Silva NRFA, Bonfante EA, Martins LM, Valverde GB, Thompson VP, Ferencz JL, *et al.* Reliability of reduced-thickness and thinly veneered lithium disilicate crowns. J Dent Res. 2012;91:305–10. https://doi.org/10.1177/0022034511433504, PMID:22205635